EJGE

Lead Adsorption in Clay and Its Application

James Adeyemo Adegoke, Ph.D.
Egbeyale Godwin Babatunde

Department of Physics, University of Ibadam, Nigeria.
e-mail: adegokeja@yahoo.com, papagoddy@yahoo.com

ABSTRACT

This work presents the adsorption capacities of some heavy metals in clay soil and its application in medical field. Nitrate of lead solution of different concentrations were prepared (400ppm, 800ppm… 6400ppm). Each concentration of lead nitrate solutions was mixed with a known volume of clay. Slabs of regular dimensions were formed from the residue after it had gone through filtration. Each slab (dried) was irradiated with x-ray radiation at different energies; 40kev, 60kev, 80kev,100kev and 120kev. Linear and mass attenuation of each slab were determined. We did this in order to check shielding ability of the adsorption capacities of heavy metals in clay soil. The research works on clay soil used mainly in building construction and pot making. A PTM UNIDOS electrometer at National Institute of Radiation Protection Research (NIRPR), University of Ibadan, was used to record the counting .A Graph of logarithm of incident intensity versus logarithm of transmitted intensity was plotted to calculate mass attenuation of the slabs at different concentrations. An Atomic absorption spectrometer (AAS) was used in analyzing the concentration of heavy metals present in each sample. The results obtained from X-ray photoelectron spectroscopy (XPS) show that attenuation coefficient decreases as the radiation energy increases. The linear correlation coefficient between the concentration of heavy metals and attenuation coefficient was approximately 1.

KEYWORDS: Attenuation, Radiation, Adsorption, Absorption, heavy metals.

INTRODUCTION

The result of the decomposition and disintegration of rocks and rock forming materials is the formation of soil. The fact that soil is so fundamental in life, it has been studied intensively for more than a century. Clay is a natural, earthy, fine grained material which develops plasticity when mixed with a limited amount of water. It is composed primarily of silica, alumina etc. (McGraw-Hill, 1989). Clay soils play vital role as medium on which plants grow. The surfaces of clay minerals are commonly charged, thereby leading to electrical neutralization. Clay minerals are known to be good adsorption materials (Fetter, 1994).

The introduction of heavy metals into soils and sediments has been studied in recent decades (Alloway, 1995, Irion and Mueller, 1987). Although many heavy metals are necessary in small amounts for biological viability, most become toxic at high concentrations. Heavy metals are often induced to the environment through modern human activities .For example, modern agricultural farming, metal mining and metallurgical processing and waste disposal has added more heavy metals to the soil.

The clay minerals, through surface ion exchange and metal-complex surface adsorption, have been studied extensively to be adsorbents of heavy metals because of their high specific surface area (Stadler and Schindler, 1993; Siantar et al., 1994; Brigatti, et al., 1996; Undabeytia, et al., 1996; Staunton and Roubaud,1997). In experimental observations, heavy metal adsorption by clays has been studied (Sposito, 1990; Frank, 1991; Davis and Kent, 1990.) to evaluate the use of clays as remedial agents in contaminated waste deposits and other areas of high heavy metal concentration (Wagner,1992).

The properties of the metal-ions (charge, ionic radius, ionic potential), as well as layer charge characteristics of the clay, including surface charge magnitude and point of origin from tetrahedral or octahedral substitution, are factors which influence adsorption selectivity (Sposito, 1989. Surface reactions in natural aqueous colloidal solutions, Chilton, 1994. The selection of previously well-characterized minerals, muscovite, illite, and montmorillonite for XPS study made it possible to relate these factors to heavy metal adsorption by the clay minerals.

The purpose of this study was to investigate the adsorption capacities of lead in clay and how it can be used in shielding ionizing radiation. X-ray photoelectron spectroscopy series PTM UNIDOS was used.

MATERIALS AND METHODS

Clay samples were collected from two States, Ekiti and Oyo, in Western region of Nigeria. In Ekiti state, samples were collected at four major locations: Isan Ekiti, Ara Ijero Ekiti, Ire Ekiti Orin Ekiti and Omi Adio in Oyo state. Samples collected were wrapped separately in a polythene bag to avoid contamination with other soil samples. This was done in other to keep the properties and identity of each sample at all stages of sample preparation constant.

Clay soils collected from different locations were turned to powdery form using pestle and mortar. The crushed clay was sieved with a sieve of size 100µm for the purpose of homogeneity for the experiment carried out. Each sample was digested using acid –acid method. Analysis of the digested samples was performed using Atomic Absorption Spectrometer. The following elements were analyzed; Cadmium, Cd, Chromium, Cr, Nickel, Ni, Manganese, Mn, Lead, Pb, Copper, Cu, and Zinc, Zn. During digestion experiment, one gram of each sample (clay) was weighed into a Teflon beaker. 10ml of conc. HNO_3 (Nitric acid) was added and it was heated. About 70% of the mixture was allowed to dry off and 10ml of hydrofluoric acid (HF) was added to the mixture and this was followed by evaporation to about 20% of the total volume. Then 5ml of Perchloric acid ($HCLO_4$) was added and the whole mixture was allowed to dry by evaporation. 1mlof HNO_3 was added to dissolve the residue and about 10ml of deionized water was added and it was allowed to boil. It was then transferred quantitatively to a 25ml standard flask and filled to the mark with deionized water. The digested samples were taken to Agronomy laboratory for chemical analysis. The results obtained were shown on Table 1. After this, slabs of dimensions 4cm x 4cm x 1cm were made when different concentrations of lead nitrate were mixed with the clay samples. Different concentration of lead nitrate prepared; 400ppm, 800ppm, 1600ppm, 3200ppm and 6400ppm. 15ml of each concentration

was added to the clay sample and mixed using a mixer. Filtration method was adopted to separate the mixture. The residue obtained was used to form the slabs. All the slabs made were oven dried in order to remove water content. All dried samples were taken to the laboratory in NIRPR and each sample was irradiated with x-ray at different energies. The result obtained was shown in the Table 2 .

RESULTS AND DISCUSSION

The result obtained from the atomic absorption spectrometer on analysis of concentration of heavy metals present in soil sample collected is presented in Table 1 below.

Table 1: Code, location and concentration of some heavy metals from selected locations

Sample Code	Location	Chromium (Cr) mg/L	Nickel (Ni) mg/L	Cadmium (Cd) mg/L	Manganese (Mn) mg/L	Lead (Pb) mg/L	Copper (Cu) mg/L	Zinc (Zn) mg/L
S1	Omi Adio	2.845	1.762	0.144	30.67	0.738	2.880	8.490
S2	Ire Ekiti	4.733	2.163	0.003	17.214	0.296	1.693	3.551
S3	Isan	2.703	1.357	0.005	20.012	1.343	0.796	4.101
S4	Orin	0.604	0.625	0.000	18.254	0.782	1.506	4.512
S5	Ara Ijero1	2.227	0.858	0.013	24.825	1.621	0.797	4.915
S6	Ara Ijero2	0.733	0.542	0.030	8.011	0.376	0.554	2.852

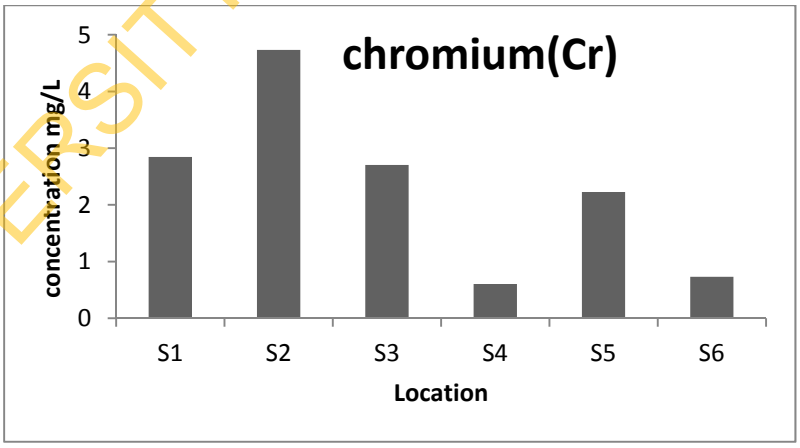

Figure 1: Bar-chart representing the concentration of Chromium in all selected areas.

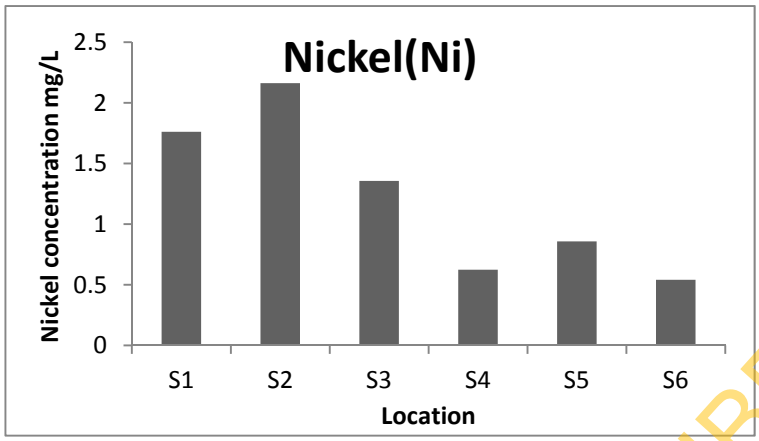

Figure 2: Bar-chart representing the concentration of Nickel in all selected areas.

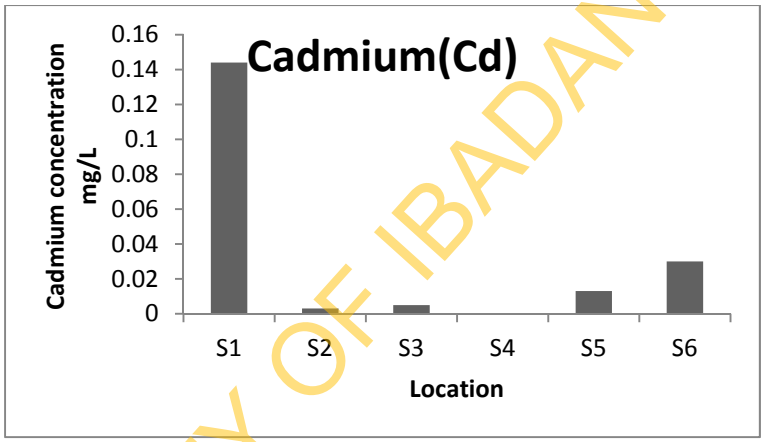

Figure 3: Bar-chart representing the concentration of Cadmium in all selected areas.

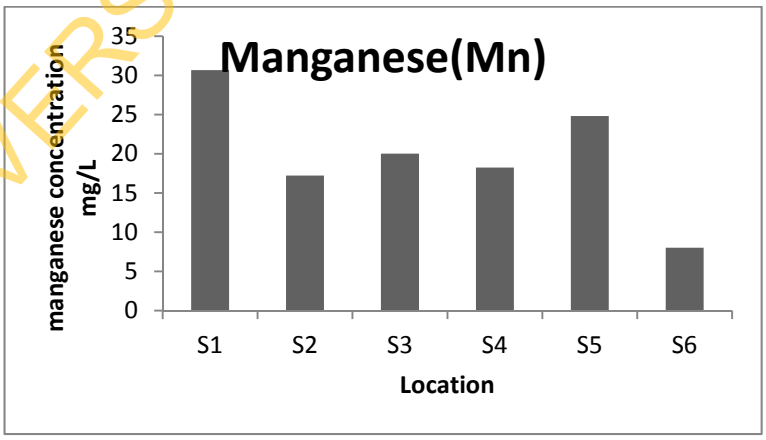

Figure 4: Bar-chart representing the concentration of Manganese in all selected areas.

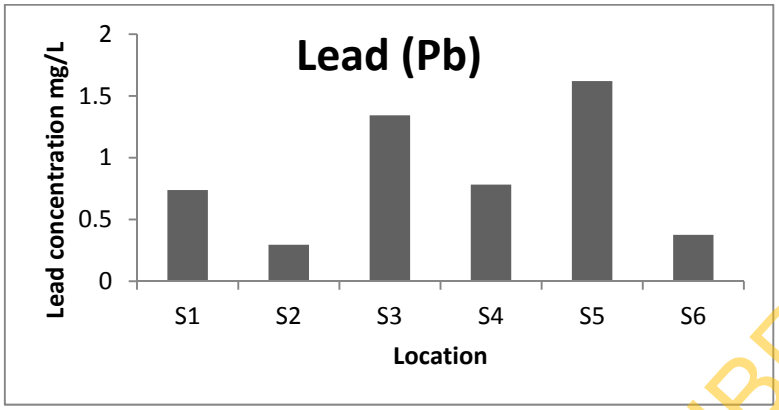

Figure 5: Bar-chart representing the concentration of Lead in all selected areas.

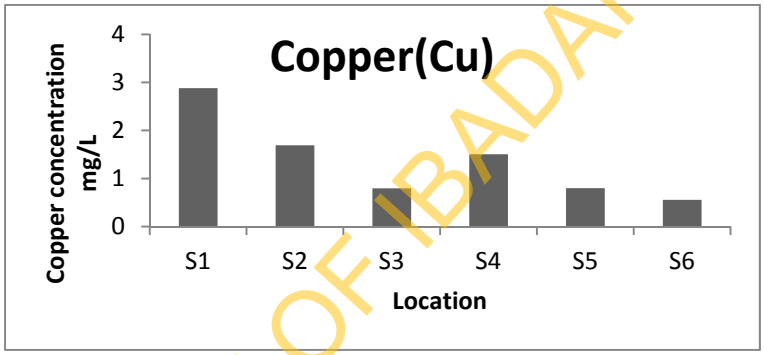

Figure 6: Bar-chart representing the concentration of Copper in all selected areas.

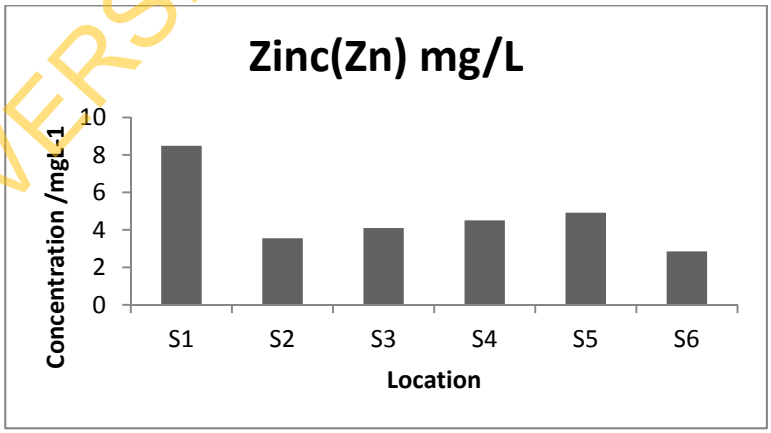

Figure 7: Bar-chart representing the concentration of Zinc in all selected areas.

DISCUSSION

Table 1 shows the result obtained when heavy metals were analyzed from the Atomic Absorption Spectrometer. Sample code S_1- S_6 was used to indicate different locations as shown in Table1.The concentration of heavy metals present in each soil sample was also presented. The table also show that sample 2 has the highest concentration of chromium followed by sample 1 and the least is sample 4.This may be due to geological formation of the soil and activities carried out in each location. Figure1 shows the bar chart of Chromium concentration at all selected areas. In this figure, sample 2 (Ire Ekiti) has the highest concentration of chromium. In Figure 2, sample from Ire Ekiti has the highest concentration of Nickel next by sample from Omiadio. In Figure 3 sample from Omi Adio has the highest cadmium concentration in all selected locations. There was no trace of cadmium from sample collected in Orin village. Figure 4 showed that Manganese was surplus in all selected clay soil samples selected. This may be due to abundant formation of Manganese in soil formation. Concentration of Lead is presented in Figure 5. It is clearly shown that all selected locations have Lead. Sample from Ara Ijero 1 has the highest concentration followed by sample from Isan and the least was sample collected at Ire Ekiti.

Calculation of attenuation coefficient

The transmitted intensity and attenuation coefficient is given below,

$$I = I_O e^{-\mu t}$$

where I = Transmitted intensity

Io = incident intensity

t = thickness of the absorbing material

μ = Linear attenuation coefficient

$$\mu = \frac{In(^{Io}/_{I})}{t}$$

Mass attenuation coefficient is calculated from the intercept of log (Io) against log(I) Graph .

log (Io) = log (I) + μt

Where μ = αρ

Log (Io) = log (I) + αρt

Therefore, $\alpha = \frac{I}{\rho t}$

Table 2: Energy at 40KeV, 10mA, Thickness = 0.01m, I_0 = 2.73

The details of the test results are extensive. The interested reader can download this document:

http://www.ejge.com/2012/ Ppr12.154_Table2.docx

Figure A1-5 shows attenuation coefficient against concentration of Lead nitrate at different energies for *sample 1*.

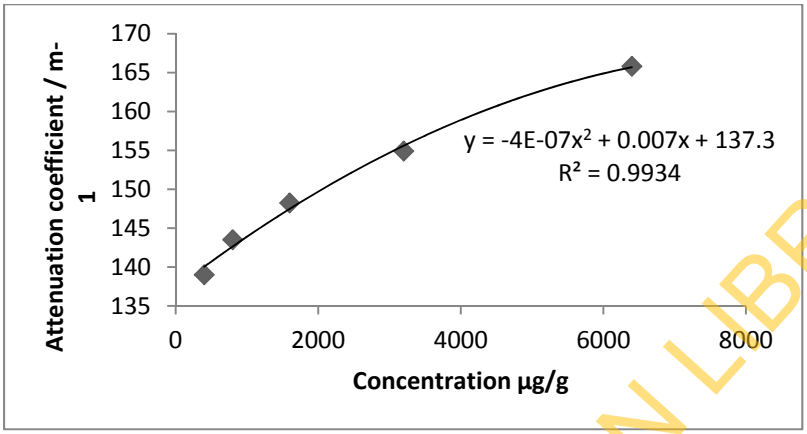

Graph 1: Attenuation coefficient against concentration of lead nitrate at 40kev.

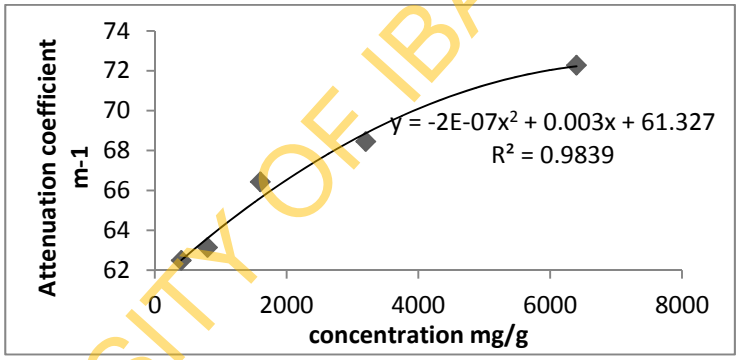

Graph 2: Attenuation coefficient against concentration of lead nitrate at 60kev.

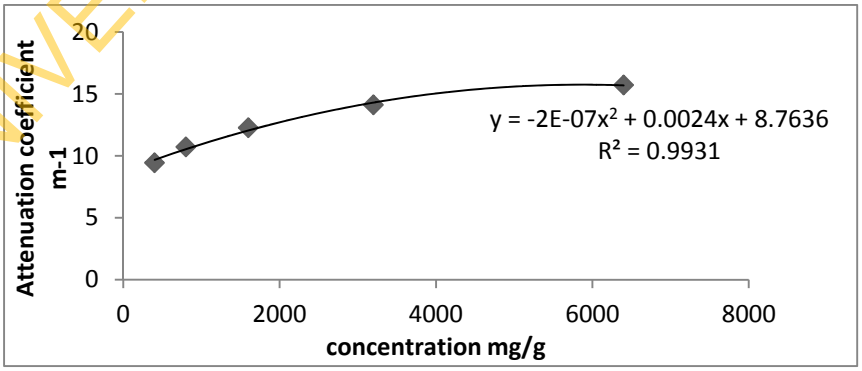

Graph 3: Attenuation coefficient against concentration of lead nitrate at 80kev.

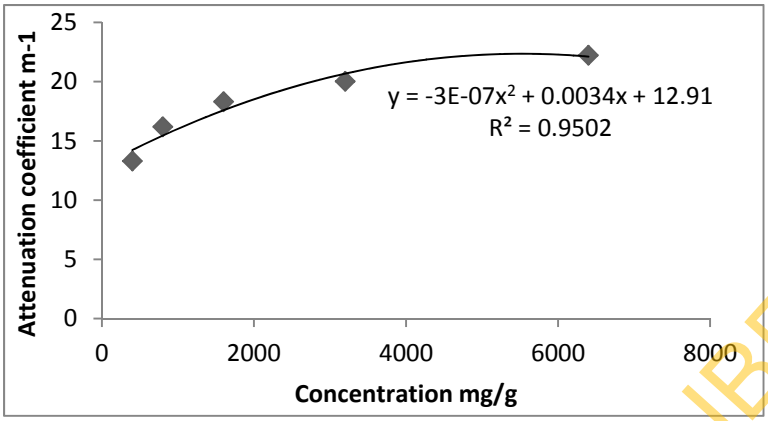

Graph 4: Attenuation coefficient against concentration of lead nitrate at 100kev.

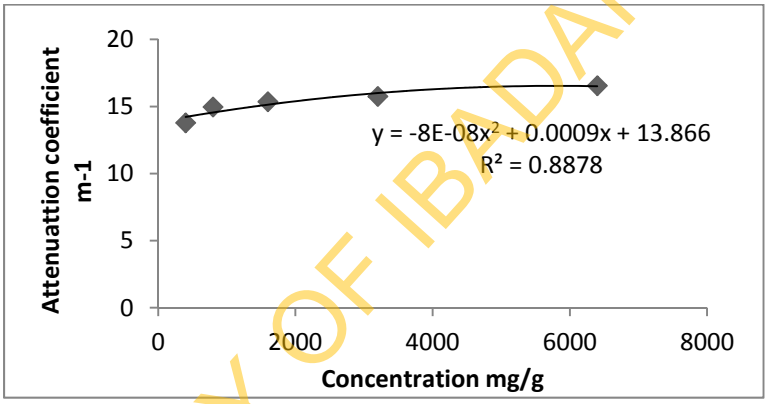

Graph 5: Attenuation coefficient against concentration of lead nitrate at 120kev.

Figures B1-5 show attenuation coefficient against concentration of lead at different energies for *sample 2:*

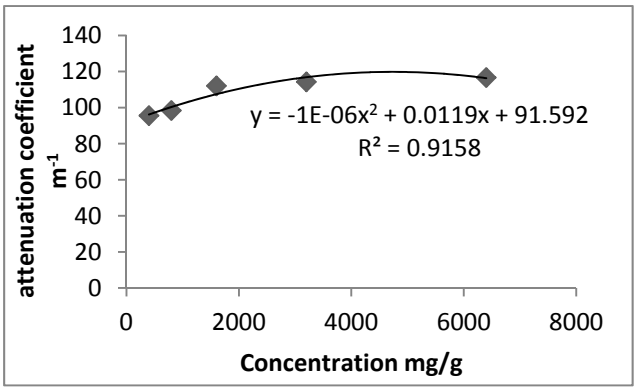

Graph B1: Attenuation coefficient against concentration of Lead nitrate at 40kev

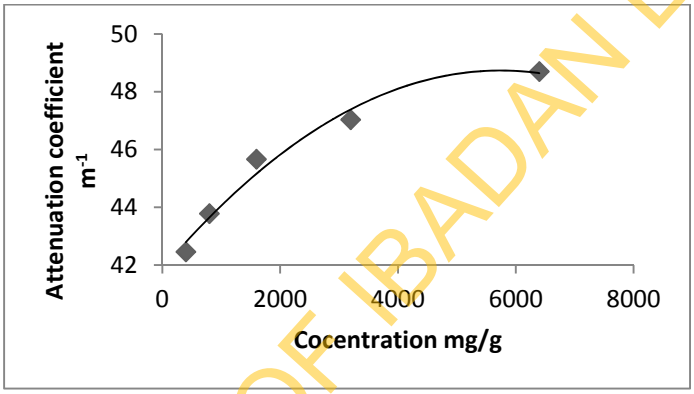

Graph B2: Attenuation coefficient against concentration of Lead nitrate at 60kev

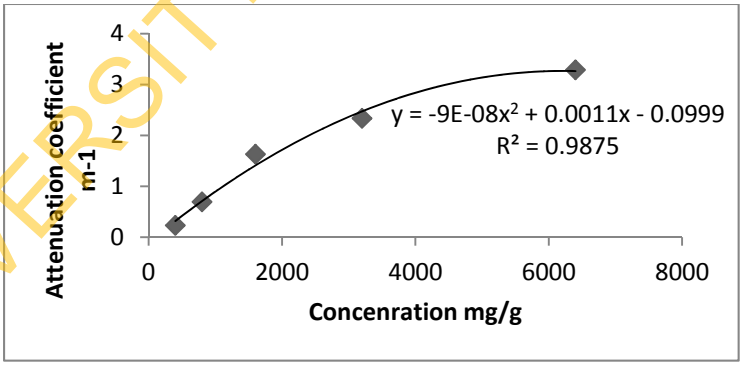

Graph B3: Attenuation coefficient against concentration of Lead nitrate at 80kev

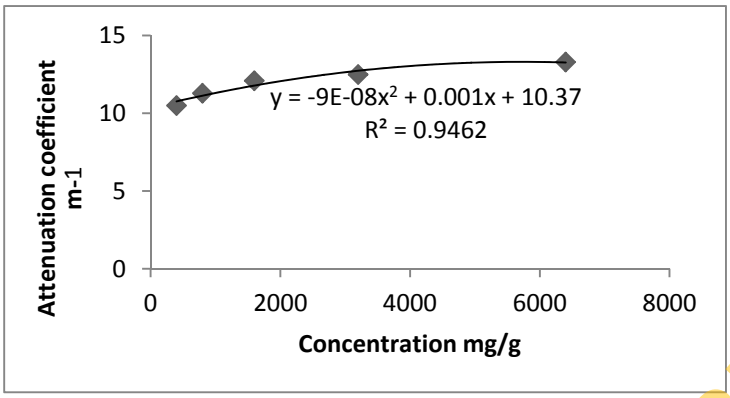

Graph B4: Attenuation coefficient against concentration of Lead nitrate at 100kev

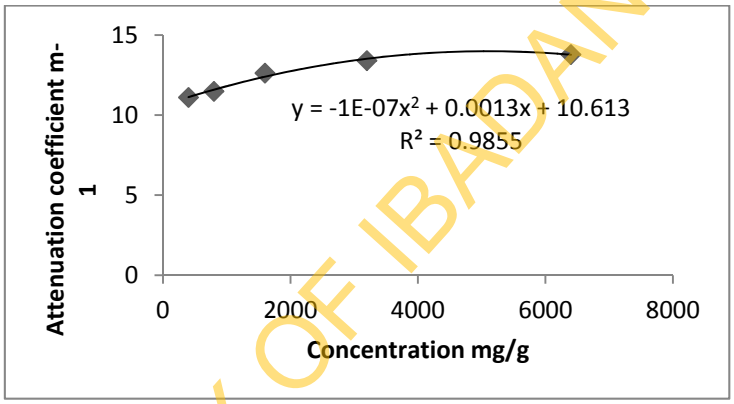

Graph B5: Attenuation coefficient against concentration of Lead nitrate at 120kev

Figures C1-5 show attenuation coefficient against concentration of Lead at different energies for *sample 3*.

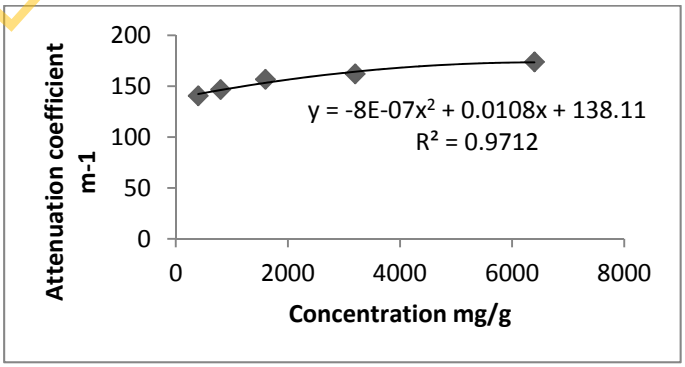

Graph C1: Attenuation coefficient against concentration of Lead nitrate at 40kev

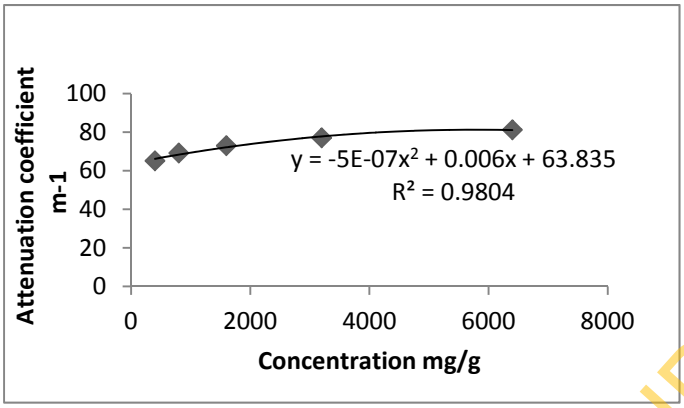

Graph C2: Attenuation coefficient against concentration of Lead nitrate at 60kev

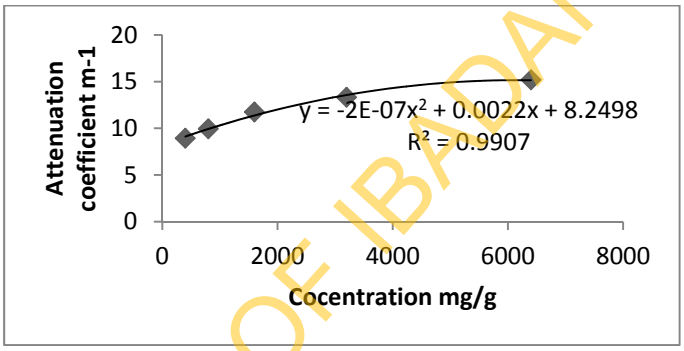

Graph C3: Attenuation coefficient against concentration of Lead nitrate at 80kev

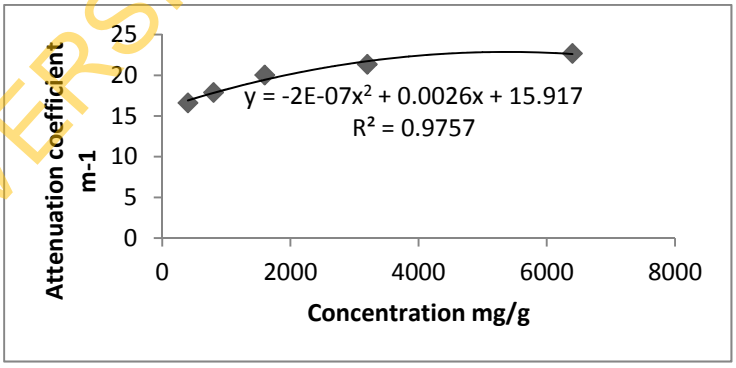

Graph C4: Attenuation coefficient against concentration of Lead nitrate at 100kev

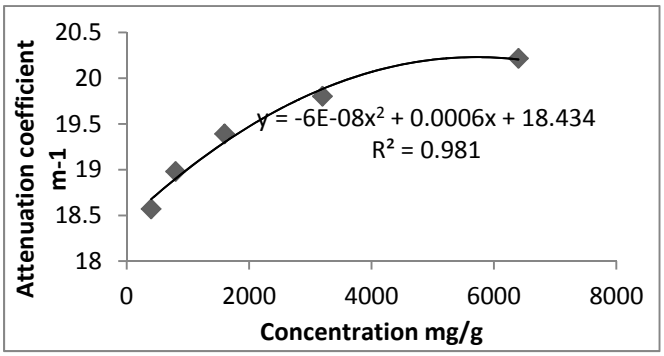

Graph C5: Attenuation coefficient against concentration of Lead nitrate at 120kev.

Figures D1-5 show attenuation coefficient against concentration of Lead at different energies for sample **4.**

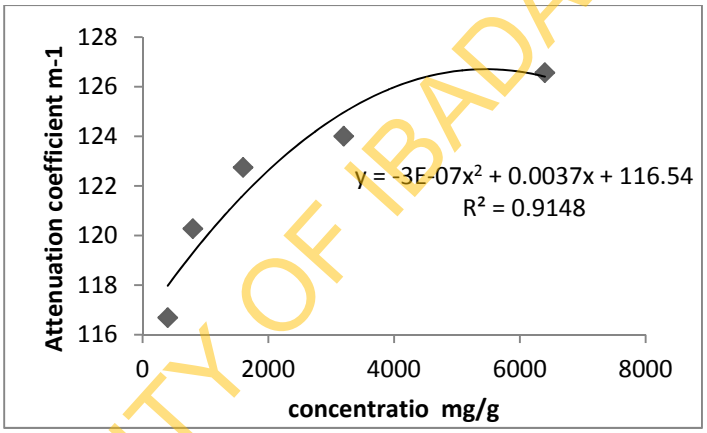

Graph D1: Attenuation coefficient against concentration of Lead nitrate at 40kev

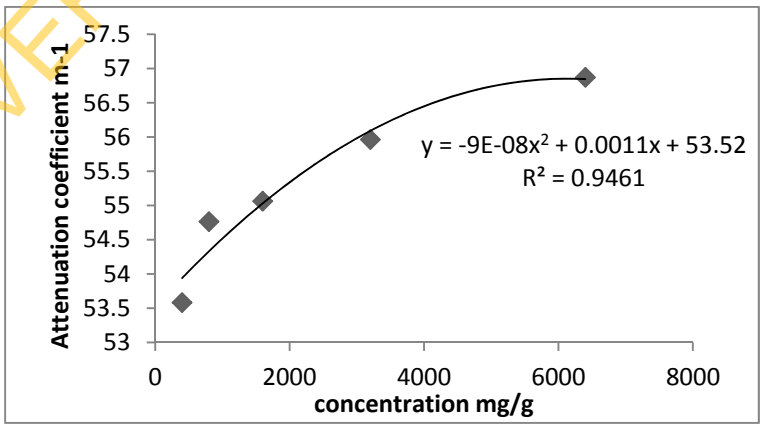

Graph D2: Attenuation coefficient against concentration of Lead nitrate at 60kev

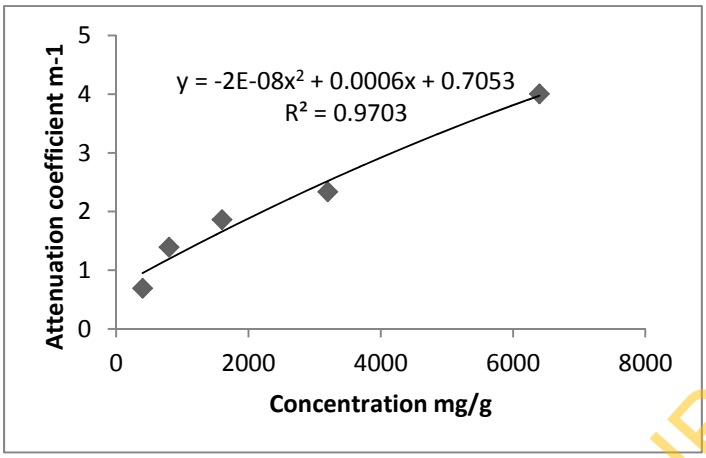

Graph D3: Attenuation coefficient against concentration of Lead nitrate at 80kev

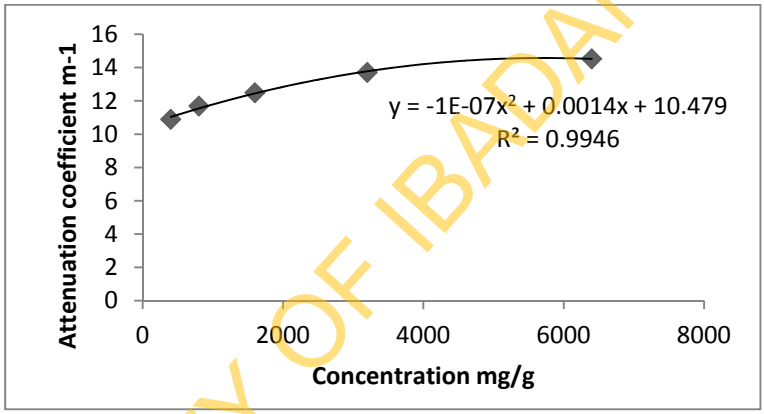

Graph D4: Attenuation coefficient against concentration of Lead nitrate at 100kev

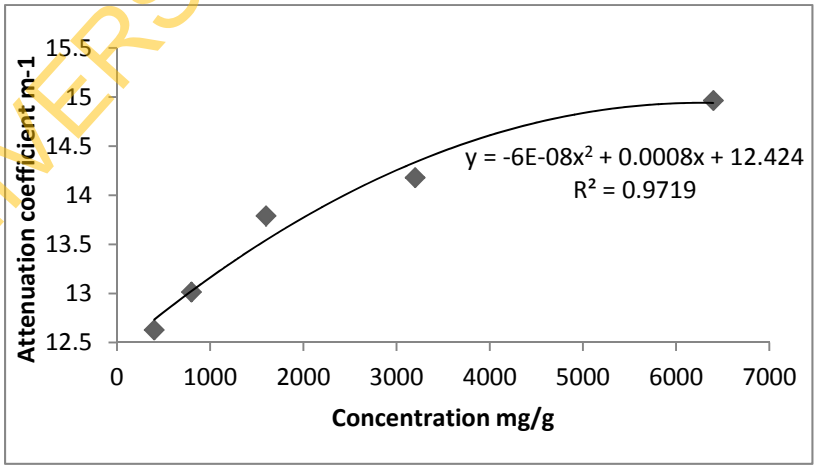

Graph D5: Attenuation coefficient against concentration of Lead nitrate at 120kev

Figures E1-5 show attenuation coefficient against concentration of Lead at different energies for *sample 5*.

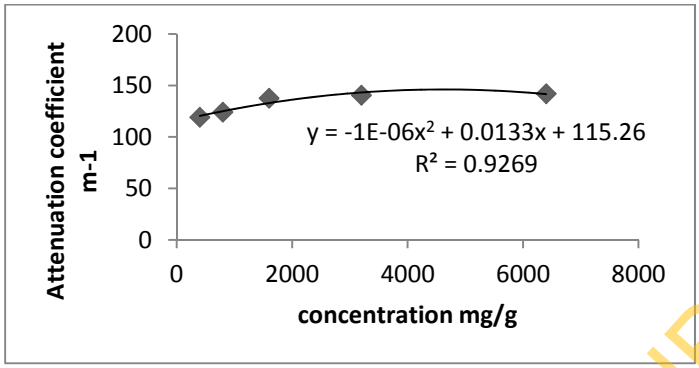

Graph E1: Attenuation coefficient against concentration of Lead nitrate at 40kev.

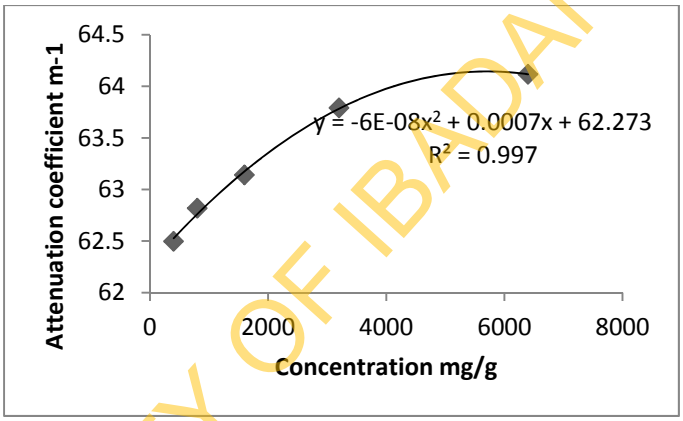

Graph E2: Attenuation coefficient against concentration of Lead nitrate at 60kev

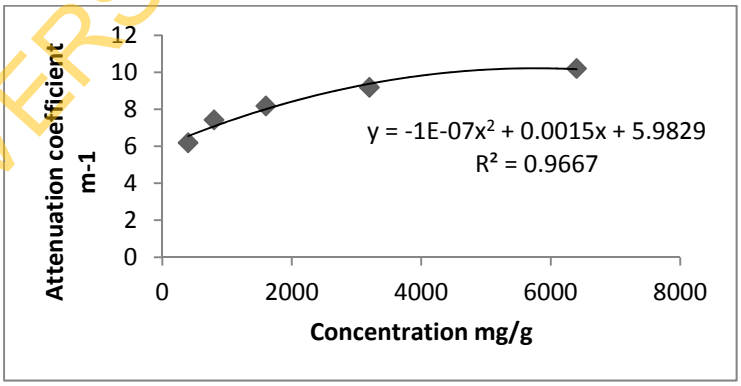

Graph E3: Attenuation coefficient against concentration of Lead nitrate at 80kev

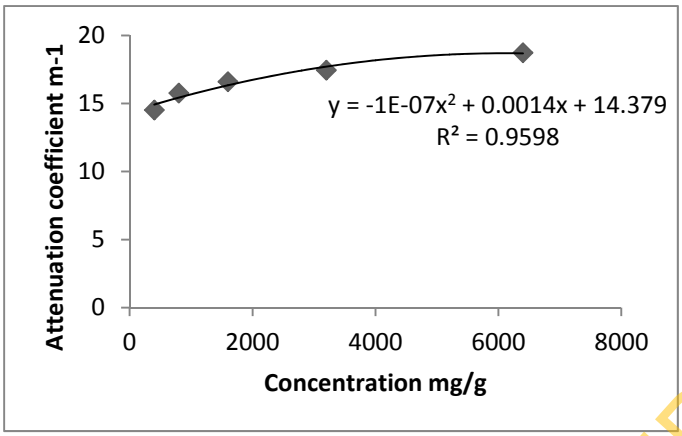

Graph E4: Attenuation coefficient against concentration of Lead nitrate at 100kev

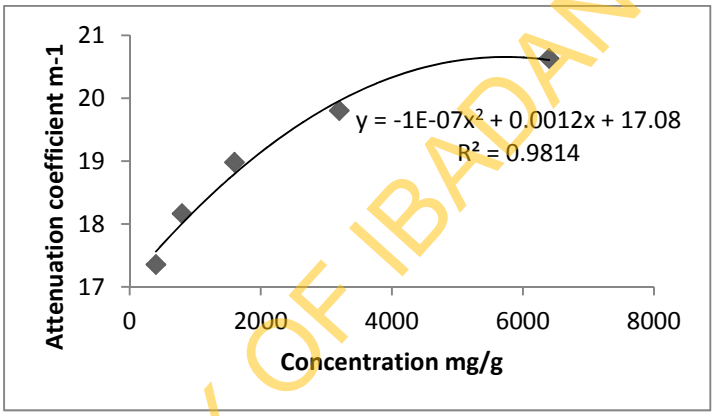

Graph E5: Attenuation coefficient against concentration of Lead nitrate at 120kev.

Table 3: logarithm of incident intensity and logarithm of transmitted intensity

At 6400ppm

log(I)	log(Io)
-0.284	0.436163
0.450249	0.764176
0.568202	0.636488
0.352183	0.448706
0.39794	0.469822

At 3200ppm

log (I)	log (Io)
-0.23657	0.436163
0.466868	0.764176
0.575188	0.636488
0.361728	0.448706
0.401401	0.469822

At 1600ppm

log (I)	log (Io)
-0.20761	0.436163
0.475671	0.764176
0.583199	0.636488
0.369216	0.448706
0.403121	0.469822

At 800ppm

log (I)	log(Io)
-0.18709	0.436163
0.489958	0.764176
0.58995	0.636488
0.378398	0.448706
0.404834	0.469822

At 400ppm

log (I)	log(Io)
-0.16749	0.436163
0.49276	0.764176
0.595496	0.636488
0.390935	0.448706
0.409933	0.469822

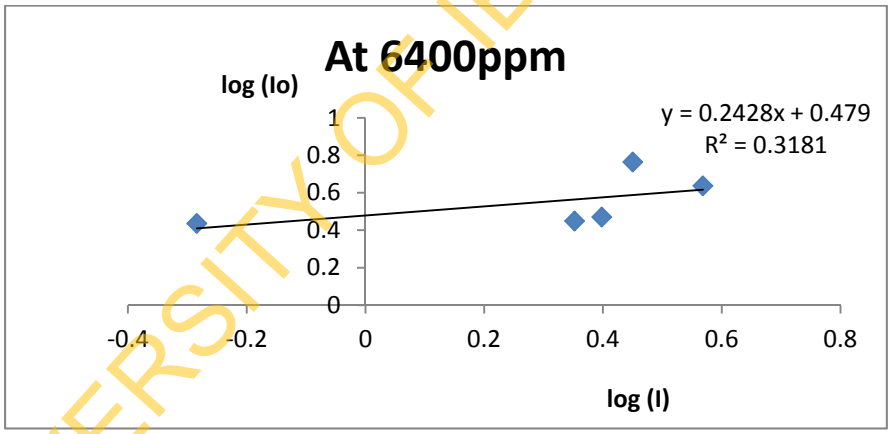

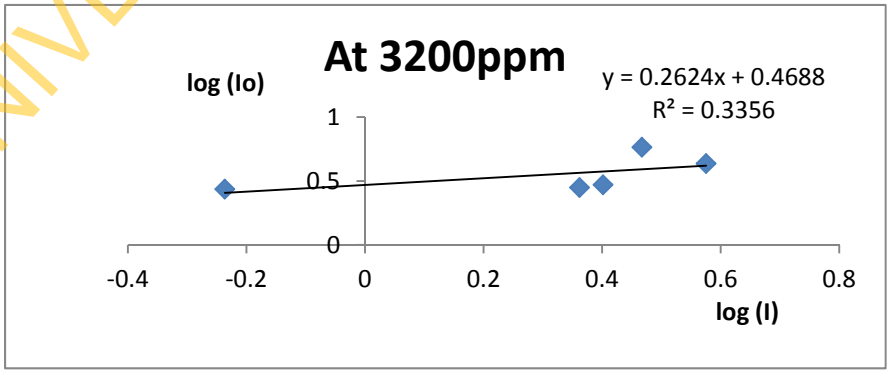

Figure continues on the next page

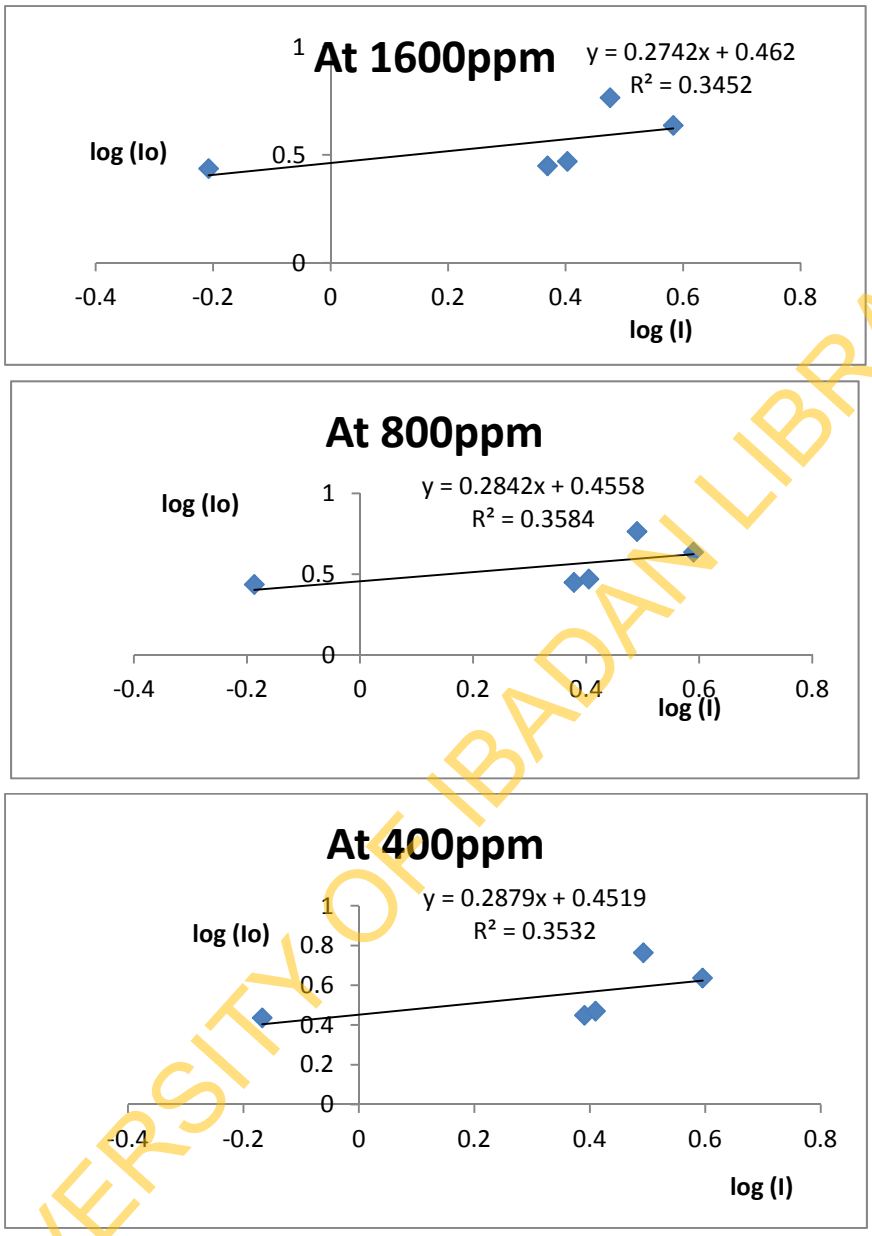

Figure F: Graph of log (Io) against log (I) at different concentration for sample 1

DISCUSSION

The linear attenuation coefficients were calculated from Lambert equation. The Graph s show exponential relationship between linear attenuation coefficient and the concentration of lead nitrate. All the samples show that as the concentration increases, there is corresponding increase in the attenuation coefficient on each sample that was irradiated. This is in agreement with general trend reported in literature review by (Dendy et al., 2003).

The linear attenuation coefficients calculated for all the samples at energy of 40Kev, 60kev, 80kev, 100kev and 120kev, current 10mA and thickness 1cm were shown in the Table2 to Table5. Table2 showed that the intensity of x-ray signal that was passed through the clay increases as the concentration of heavy metal (lead) ion adsorbed by the clay decreases. The results in Table 2a-Table 2e showed the same trend.

Table 2 shows the result obtained for sample 1to sample 6 when the X-ray machine was set at the energy 60KeV and current 10mA. The attenuation coefficient decreases as the concentration in each sample decreases. This shows that intensity of the radiation increases as concentration decreases in each sample. This is also represented by the Graph shown in Graph A2, B2 and C2. From the observation discussed above, it can be said that the interaction in clay material depends on adsorption of heavy metal ion. The increase in concentration of nitrate of heavy metals caused reduction in intensity of the radiation (Salinas et al 2006)

Table 2 shows that Sample 3 has the highest attenuation coefficient followed by Sample 1 and next by Sample 6, the least is Sample 2. This implies that Clay sample obtained from Isan in Ekiti state is the best material in shielding ionizing radiation when compared with other samples collected. Clay sample collected from ire in Ekiti State is the least material in shielding ionizing radiation among other samples. The greater the attenuation coefficient the better is the material for shielding ionizing radiation (Davidson et al., 1991).

Figures A1-5 show the attenuation coefficient against concentration of Lead for sample 1. FigureA1 Graph s showed that attenuation coefficient increases as the concentration of Lead increases.FigureA2 shows that attenuation coefficient increases as the concentration of Lead ion increases and the attenuation almost reaches its peak at certain concentration. This implies that the samples containing solutions of different concentration of Lead (ii) ions continue to adsorb the Lead, Pb, ions from the solution without reaching the saturation level. The slope of the Graph decreases as the concentration increases. This means that further increase in concentration, attenuation will tend to be constant at certain value. The Graph in Figure A4 and A5 showed that attenuation increases as the concentration of Lead ion increases and the attenuation reaches its peak at concentration between 5800ppm and 6200ppm. FigA1-5 shows that the slope of the Graph decreases as the energy on sample 1 increases.

Graph B1-5 show the attenuation coefficient against concentration of Lead ion for sample 2.The Graph s showed the same trend .The attenuation coefficient in clay sample 2 reached maximum value at range 5000ppm. Figure (A-E) show similar trend in adsorption capacity.

Figure E shows the Graph of logarithm of incident intensity against logarithm of transmitted intensity. The intercept of this Graph was used to calculate mass attenuation coefficient .At concentration 6400ppm, 3200ppm, 1600ppm, 800ppm and 400ppm mass attenuation coefficient was 0.256699, 0.251233, 0.247588, 0.244266 and 0.242176 respectively. The intercept of the Graph decreases as the concentration decreases. This implies that high concentration of lead in a clay slab would be good for X-ray shielding.

CONCLUSION

From the work carried out, Heavy metals present in the clay samples were determined. The results are presented on Table1. Linear attenuation coefficient was calculated from the results obtained with XPS. The Graph of linear attenuation against concentration of Lead ion are shown on Figure A-E. The radiation effect of adsorption capacity of lead ions in clay at different locations, Omi Adio and Ekiti state, was determined and shown on Table 2 – Table 6. The result obtained on Table 2

shows greater attenuation coefficient value than others. An Atomic absorption spectrometer (AAS) was used in analyzing the concentration of heavy metals present in each sample. The results show that Manganese was the most prominent metal found in the clay followed by Zinc and next by Lead in our area of study. The results obtained from X-ray photoelectron spectroscopy (XPS) show that attenuation coefficient decreases as the energy of ionizing radiation increases. Graph s of attenuation coefficient was plotted against the concentration of Lead. The linear correlation coefficient between the concentration of heavy metals and attenuation coefficient was approximately 1. The mass attenuation was also calculated from the Graph of logarithm of incident intensity against logarithm of transmitted intensity.

ACKNOWLEDGEMENTS

We gratefully acknowledge permission to use the AAS (Atomic Absorption Spectrophotometer, Buck Scientific Model 210VGP) in the Department of Agronomy, university of Ibadan for heavy metal determination and NIRPR in the department of radiology, university of Ibadan for testing attenuation at narrow beam. Especially helpful in collecting and interpreting XPS data were Mr. Akerele and Mr. Ayuba.

REFERENCES

1. Alloway, B.J., 1995. Heavy Metals in Soils. 2nd ed. Blackie Academic & Professional, London.
2. Brigatti,M.F, Campana, G., Medici L. and Poppi L. (1996) .The influence of layer-charge Zn (II) sorption by smectites. Clay min. pg 477-483
3. Chilton A.B, Shultis J.K. and Faw R.E. (1984).Principles of Radiation Shielding, New Jersey Prentice-Hall,Inc.
4. Davidson, N., McWhinnie, W.R., Hooper, A., 1991. X-ray photoelectron spectroscopic study of cobalt _II. and nickel _II. sorbed on hectorite and montmorillonite. Clays Clay Miner. 39, 22–27.
5. Davis, J.A. and Kent, D.B., 1990. Surface complexation modeling in aqueous geochemistry. In: Hochella, M.F., White, A.F. _Eds.., Mineral-Water Interface Geochemistry. Rev. Mineral. Vol.23, pp. 177–260.
6. Dendy, P.P and Heaton B. (2003). Physics for Diagnostic Radiology,(2nd ed). Bristol and Philadelphia;Institute of physics Publishing.
7. Fetter C.W (1994) . ‘‘Applied Hydrogeology’’ (3rd ed.) Macmillan College Pub.,New York. Pg 691.
8. Frank, K., 1991. Tongesteine: Retention von Schwermetallen und die Einflussnahme kuenstlicher Komplexbildner. Schriftenr. Angew. Geol. Karlsruhe 11, 249 pp.
9. Irion, G.and Mueller, G., 1987. Heavy metals in surficial sediments of the North Sea. In: Proc.
10. Intern. Conf. on Heavy Metals in the Environment, New Orleans, 1987. pp. 38–41.
11. McGraw-Hill Dictionary of scientific and technical terms by Parker(1989), 4th edition. Sybil P. Parker (editor- in- chief). New York St. Louis San Francisco pp 362, 539, 868,

1784.

12. Salinas, I.C.P; Conti, C.C; Lopes, R.T. (2006) Effective density and mass attenuation coefficient.
13. Siantar D.P., Feinberg B.A. and Fripiat J.J. (1994) Interaction between organic and inorganic pollutants in the clay interlayer. Clays min. pp 187-196.
14. Sposito G., 1990. Molecular models of ion adsorption on mineral surfaces. In: Hochella, M.F.,
15. White, A.F. _Eds.., Mineral-Water Interface Geochemistry. Rev. Mineral. 23 pp. 261–279.
16. Stadler M. and Schindler P.W. (1993). The effect of dissolved ligands upon the sorption of Cu (II) by Ca-montmorillonite.Clays min. pp. 680-692.
17. Staunton S. and Roubaud M. (1997). Adsorption of Cs-137 on montmorillinite and illinite: Effect of charge compensation cation, ionic strength, concentration of Cs, K and fulviic acid. Clays min. pp. 251-260.
18. Undabeytia T.,Morillo E. and Maqueda C. (1996). Adsorption of Cd and Zn on Montmorillonite in the presence of a cationic pesticide. Clays Min. pp.485-490.
19. Wagner, J.F., 1992. Verlagerung und Festlegung von Schwermetallen in tonigen Deponieabdichtungen.Ein Vergleich von Labor- und Gelaendestudien. Schriftenr. Angew. Geol. Karlsruhe 22, 1–246.